

Orthostatic tremor: a cerebellar pathology?

Cécile Gallea,^{1,2,3,4,5} Traian Popa,^{1,2,3,4} Daniel García-Lorenzo^{1,2,3,4,5}
 Romain Valabregue,^{1,2,3,4,5} André-Pierre Legrand,⁶ Emmanuelle Apartis,^{2,3,4,7}
 Lea Marais,^{1,2,3,4,5} Bertrand Degos,^{2,3,4,8} Cecile Hubsch,^{2,3,4,8} Sara Fernández-Vidal,^{1,2,3,4}
 Eric Bardinet,^{1,2,3,4} Emmanuel Roze,^{2,3,4,8} Stéphane Lehéricy,^{1,2,3,4,5} Sabine Meunier^{2,3,4,*}
 and Marie Vidailhet^{2,3,4,8,*}

*These authors contributed equally to this work.

See Muthuraman *et al.* (doi:10.1093/aww164) for a scientific commentary on this article.

Primary orthostatic tremor is characterized by high frequency tremor affecting the legs and trunk during the standing position. Cerebellar defects were suggested in orthostatic tremor without direct evidence. We aimed to characterize the anatomo-functional defects of the cerebellar motor pathways in orthostatic tremor. We used multimodal neuroimaging to compare 17 patients with orthostatic tremor and 17 age- and gender-matched healthy volunteers. Nine of the patients with orthostatic tremor underwent repetitive transcranial stimulation applied over the cerebellum during five consecutive days. We quantified the duration of standing position and tremor severity through electromyographic recordings. Compared to healthy volunteers, grey matter volume in patients with orthostatic tremor was (i) increased in the cerebellar vermis and correlated positively with the duration of the standing position; and (ii) increased in the supplementary motor area and decreased in the lateral cerebellum, which both correlated with the disease duration. Functional connectivity between the lateral cerebellum and the supplementary motor area was abnormally increased in patients with orthostatic tremor, and correlated positively with tremor severity. After repetitive transcranial stimulation, tremor severity and functional connectivity between the lateral cerebellum and the supplementary motor area were reduced. We provide an explanation for orthostatic tremor pathophysiology, and demonstrate the functional relevance of cerebello-thalamo-cortical connections in tremor related to cerebellar defects.

1 Centre de NeuroImagerie de Recherche – Institut du Cerveau et de la Moelle épinière, ICM, Paris, France

2 Sorbonne Universités, UPMC Univ Paris 06, UMR S 1127, Paris, France

3 CNRS, UMR 7225, Paris, France

4 Inserm, U 1127, Paris, France

5 AP-HP, Hôpital de la Pitié Salpêtrière, Département de Neuroradiologie, Paris, France

6 ESPCI, Paris Sciences, Paris, France

7 AP-HP, Hôpital de Saint-Antoine, Département de Neurologie, Paris, France

8 AP-HP, Hôpital de la Pitié Salpêtrière, Département de Neurologie, Paris, France

Correspondence to: Cecile Gallea, Centre de Neuroimagerie de Recherche – CENIR, Institut du Cerveau et de la Moelle épinière – ICM, Groupe Hospitalier Pitié-Salpêtrière, 75651 Paris, cedex 13 France

Keywords: cerebellar function; motor cortex; movement disorder; tremor; frontal lobe

Abbreviations: ALFF = amplitude of low frequency fluctuation of blood oxygen level-dependent signal; DMN = default mode network; FAB = Fullerton Advanced Balance rating scale; M1 = primary motor cortex; TMS = transcranial magnetic stimulation; SMA = supplementary motor area; VBM = voxel-based morphometry

Received January 13, 2016. Revised March 29, 2016. Accepted April 22, 2016. Advance Access publication June 21, 2016

© The Author (2016). Published by Oxford University Press on behalf of the Guarantors of Brain. All rights reserved. For Permissions, please email: journals.permissions@oup.com This is an Open Access article distributed under the terms of the Creative Commons Attribution Non-Commercial License (<http://creativecommons.org/licenses/by-nc/4.0/>), which permits non-commercial re-use, distribution, and reproduction in any medium, provided the original work is properly cited. For commercial re-use, please contact journals.permissions@oup.com

Introduction

Primary orthostatic tremor is a rare condition characterized by singular symptoms including a high frequency 13–18 Hz tremor of the legs and trunk that appears in the standing position, and which is associated with a strong feeling of instability, fear of falling, fatigue, and often pain (Thompson *et al.*, 1986; Deuschl *et al.*, 1998; Gerschlager *et al.*, 2004; Piboolnurak *et al.*, 2005; Mestre *et al.*, 2012; Yaltho and Ondo, 2014; Ganos *et al.*, 2016). Subjective unsteadiness worsens over time, while posturographic measurements reveal an increase of the total sway path without concomitant change of the tremor frequency (Ganos *et al.*, 2016). Whether impaired balance control is the consequence of a pathological orthostatic tremor (Fung *et al.*, 2001) or whether the tremor is the response to a primarily abnormal control of balance (Sharott *et al.*, 2003) is still under debate. This latter hypothesis came from the finding that, in healthy humans, postural instability caused by galvanic stimulation or leaning backwards elicited coherent EMG bursts at ~ 16 Hz (Sharott *et al.*, 2003), similar to the orthostatic tremor frequency.

Cerebellar dysfunction in orthostatic tremor has been suggested (Feil *et al.*, 2015), but was never directly demonstrated. Indeed, the increase of total sway path, the presence of a second frequency peak at 3–5 Hz—the usual frequency of cerebellar tremor—point toward cerebellar dysfunction in orthostatic tremor (Ganos *et al.*, 2016). In addition, orthostatic tremor was found in some patients with lesions of the cerebellum or the pons (Benito-León *et al.*, 1997; Setta and Manto, 1998; Setta *et al.*, 1998). This raises another question related to the nature of the cerebellar network dysfunction, whether it would be specific to orthostatic tremor given the singularity of the symptoms, or whether it would share cerebellar dysfunction with other pathological tremors like essential tremor (Schnitzler *et al.*, 2009; Gallea *et al.*, 2015) or parkinsonian tremor (Timmermann *et al.*, 2003). The few neuroimaging studies performed in orthostatic tremor (Wills *et al.*, 1996; Guridi *et al.*, 2008) do not clearly answer this question. In a single case study using fluorodeoxyglucose (FDG)-PET, a patient with a orthostatic tremor had bilateral primary motor cortex and cerebellar vermis hypermetabolism, which returned to normal when the tremor was suppressed by deep brain stimulation of the ventral intermediate nucleus of the thalamus receiving cerebellar inputs (Guridi *et al.*, 2008). In the same line of evidence, bilateral stimulation of the ventral intermediate nucleus partially improved orthostatic tremor in other studies (Espay *et al.*, 2008; Guridi *et al.*, 2008; Magariños-Ascone *et al.*, 2010; Yaltho and Ondo, 2011; Lyons *et al.*, 2012; Contarino *et al.*, 2015). Yet the improvement was less obvious than in essential tremor, suggesting that the pathophysiology of orthostatic tremor and essential tremor engages different parts of the cerebellar motor loops or different pathways. The other

potential oscillators proposed in orthostatic tremor are in the centres regulating stance and tone located in the brainstem (Wu *et al.*, 2001; Kızıltan *et al.*, 2012), and in spinal cord (Norton *et al.*, 2004). A self-escalating deleterious cycle between proprioceptive feedback and tremor might also participate in orthostatic tremor: the tremor degrades the proprioceptive afferent feedback from the legs, which triggers an increase of muscle contraction to stabilize the lower limbs, eventually resulting in tremor worsening (Fung *et al.*, 2001).

The first aim of this study was to characterize, in orthostatic tremor, the structural and functional defects in the cerebellar motor pathways, particularly those involved in postural control. To that end, we used voxel-based morphometry, and resting-state functional MRI to analyse the amplitude of low frequency fluctuations (ALFF) of the blood oxygen level-dependent (BOLD) signal. The fluctuations of resting-state BOLD signals are generally observed to be present between 0.01 and 0.08 Hz frequency band (Biswal *et al.*, 1995), and the amplitude is reported for these low frequency fluctuations (Yang *et al.*, 2007). Recent studies have observed an overlap between changes in regional ALFF and functional connectivity in several brain regions (Xuan *et al.*, 2012), suggesting that ALFF reflects changes of neural activity. Changes in ALFF in the cerebello-thalamo-cortical network were observed in patients with essential tremor compared to healthy controls (Gallea *et al.*, 2015). Altogether, this suggests that ALFF is a meaningful tool to investigate network disorders. We compared 17 patients with orthostatic tremor with homogeneous symptoms in the lower limbs and 17 age- and gender-matched healthy volunteers. The second aim was to assess the relationship of functional neuroanatomical changes of the cerebellar motor pathways with the clinical and electrophysiological characteristics of tremor. In a subgroup of nine patients, we tested the functional relevance of the long-range connections between the cerebellum and both the primary and secondary motor areas. To that end we modulated the cerebellar activity using repeated sessions of repetitive transcranial magnetic stimulation (TMS) of the cerebellum to measure its impact on the clinical scores, electrophysiological recordings and resting state functional connectivity in the cerebellar motor pathways.

Materials and methods

Study design

This study includes (i) a neuroimaging study aiming to describe the neuronal network involved in orthostatic tremor; and (ii) an open label trial combining repetitive TMS and functional MRI recordings aiming to test the modulation of this network through cerebellar external stimulation.

Table 1 Characteristics of the patients

	Age (y)	Age at onset (y)	FAB	Duration of upright position	F	W	A	Medication
TO1	74	64	28	120	14.34	0.295	8.16	No
TO2	71	52	35	330	16.75	0.325	3.015	Rivotryl
TO3	69	52	28	150	16.2	0.4	1.55	Rivotryl
TO4	62	53	27	65	14.08	0.31	0.035	Rivotryl
TO5	52	42	24	55	17.7	0.4	6.2	Rivotryl
TO6	60	49	25	0	13.555	0.295	1.935	No
TO7	58	42	28	84	16.125	0.335	2.48	Rivotril
TO8	58	44	19	14	17.885	0.47	0.35	Rivotril
TO9	79	62	24	111	15.64	0.32	1.5	Rivotril
TO10	78	44	29	90	16.885	0.378	0.142	Rivotril
TO11	67	56	31	83	15.288	0.518	1.016	No
TO12	66	61	16	35	17.169	0.710	1.150	Rivotril
TO13	38	27	34	180	16.120	0.291	0.358	No
TO14	60	51	17	120	16.440	0.485	2.948	No
TO15	68	67	33	210	14.102	0.555	1.167	Rivotril
TO16	47	39	38	187	15.714	0.319	0.237	Rivotril
TO17	77	70	23	285	17.199	0.562	0.848	Rivotril
Average	63.765	51.471	27.00	124.647	15.952	0.410	1.947	
SD	10.871	10.895	6.019	88.052	1.273	0.117	2.137	

W = width of the power spectrum; A = area under the curve; F = frequency peak value; SD = standard deviation.

Subjects

Neuroimaging study

We enrolled 17 patients with orthostatic tremor (12 females and five males; aged 63 ± 10.5 years) and 17 healthy volunteers matched for age and gender (12 females and five males; aged 62.7 ± 11.2 years). All subjects underwent a clinical assessment and a neuroimaging protocol. The diagnosis of orthostatic tremor was based on the Movement Disorders Consensus Criteria (Deuschl *et al.*, 1998). Clinical characteristics of the patients are reported in Table 1. All the patients had prominent bilateral lower limbs orthostatic tremor with a tremor frequency within the 13–18 Hz, in the lower limbs and coherence between the two legs (Table 1). None of the participants had any neurological problem apart from orthostatic tremor for the patients. All patients but five were taking low dose (<1.5 mg) clonazepam at the time of the study. Patients were also tested for global cognitive capabilities [Mini-Mental State Examination (MMSE)] and for quality of life (SF36). All the participants gave their written informed consent. The protocol was approved by the local ethics committee.

Repetitive transcranial magnetic stimulation trial over the cerebellum

Nine (six females, mean age 64.8 ± 7.5 years, range 52–79) of the 17 patients of the main study participated in an open label trial aiming to influence the functional connectivity between the cerebellum and the thalamo-cortical components of the cerebello-thalamo-cortical network. Fifteen minutes of repetitive TMS were delivered daily for five consecutive days over each cerebellar hemisphere. The first stimulation session took place after completion of the clinical examination and imagery protocol of the main study. The clinical assessment, electrophysiological quantification of tremor and imagery protocol were repeated right after the last stimulation (Day 5).

Clinical assessment and electrophysiological quantification of tremor were also performed during two follow-up sessions 12 (Day 12) and 26 (Day 26) days, respectively, after the first stimulation session.

The procedure for cerebellar stimulation has already been used in patients with essential tremor (Popa *et al.*, 2013) and will be only summarized here. The first step was to calculate the resting motor threshold (RMT), defined as the minimum stimulus intensity that resulted in motor-evoked potentials of 50 μ V in at least 5 of 10 trials in the right first dorsal interosseus muscle. In a second step, repetitive TMS was delivered, under neuronavigation (Nextim Ltd), daily for five consecutive days over the lobule VIII of each cerebellar hemisphere, using a figure-of-eight coil connected to a RapidStim2 machine (Magstim). Nine-hundred pulses were delivered consecutively to each side with a frequency of 1 Hz and at an intensity of 90% of the RMT for a total duration of 15 min for each cerebellar hemisphere.

Clinical examination and evaluation of orthostatic tremor

The clinical assessment was performed by a movement disorders specialist (E.R.) using the Fullerton Advanced Balance (FAB) rating scale (Rose *et al.*, 2006), designed to evaluate postural instability. Lower scores were associated with greater postural stability. We also measured the duration that the patients could maintain upright station. Patients answered three questionnaires related to their postural instability and fear of falling: (i) the Falls Efficacy Scale-International (FES-I); (ii) the Survey of Activities and Fear Of Falling in the Elderly (SAFFE); and (iii) the Consequences of Falling (COF).

Electrophysiological quantification of tremor was performed from electromyographic (EMG) recordings of the tibialis anterior muscles. EMG signals were recorded during two 30-s

sessions of active upright station. All identifiable information was removed from the EMG files and replaced with a code known only to the principal investigator (S.M.). The EMG data were analysed by an expert physicist (A.P.L.), blinded to the subjects identity and status. The EMG signals were analysed in frequency space and characterized by the peak frequency (F), area (A), and width (w) of a Gaussian curve fitting the tremor peak of the power spectrum. Area is considered to reflect the tremor severity and width the frequency dispersion.

Statistical analysis of clinical scores and electrophysiological measures of tremor

The scores at the FAB rating scale (postural instability impairment), the maximum duration of upright station that patient could maintain, the disease duration, and the three EMG values quantifying tremor (F, A and w) were considered for correlations with the MRI findings using a multiple regression analysis (see 'Data analysis and statistics' section).

To evaluate the effect of cerebellar repetitive TMS on tremor severity, all the clinical and electrophysiological measures at Days 5, 12 and 26 were compared to Day 0 (baseline, performed before the beginning of repetitive TMS treatment) using a repeated measure ANOVA.

Neuroimaging study

Data acquisition

MRI data were collected on a Siemens 3 T MAGNETOM Trio equipped with a 12-channel head coil. We first acquired high-resolution T_1 -MPRAGE images (repetition time/echo time/flip angle = 6.2 s/3 ms/9°, 1 mm³ isotropic voxel size, field of view = 256 × 256 × 176 mm, 144 sagittal images). Resting state functional images were acquired by T_2^* -weighted fast echo planar imaging (repetition time/echo time/flip angle = 3.3 s/30 ms/90°, voxel size = 1.5 × 1.5 × 2.5 mm, 200 volumes acquired per subject) from 46 interleaved axial slices. The resting state functional MRI experiment consisted of a 10-min run in which participants were asked to relax with their eyes closed, without falling asleep. A field map was acquired to correct for echo planar image distortions induced by each subject's individual magnetic susceptibilities. A quality control was systematically performed on the MRI data. In this control, we verified the wrapping or ghosting in the anatomical images. In addition, for the functional images, we verified the presence of susceptibility artefacts, spiking, ringing, or motion slice artefacts. All images with head motions superior to 3 mm during resting state were excluded from the analysis.

Data analysis and statistics

We first looked for structural differences in grey matter between the patients and controls by using voxel-based analyses (voxel-based morphometry, VBM), both in the whole brain and in specific regions of interest. Second, we looked for functional differences in regions of interest of the cerebello-thalamo-cortical network using ALFF analysis. Third, we looked for differences in functional connectivity in the cerebello-thalamo-cortical network, considering regions that showed

significant structural and/or functional differences between patients and matched controls. Finally, we asked whether clinical and electrophysiological variables correlated with grey matter volume, ALFF and functional connectivity levels in the cerebello-thalamo-cortical network. Individual intake of clonazepam was systematically entered as a nuisance co-variable in the VBM and functional MRI analyses.

To verify the specificity of the correlations as being related to orthostatic tremor, we investigated whether other variables not directly related to tremor would be associated with structural and functional measures in the cerebellum and in the cortical motor areas. These other variables included the scores at MMSE, SF36, SAFFE, FES-I and COF.

Regions of interest

We used atlases to define regions of interest containing the cerebellar and brain regions of the involved in voluntary motor control of the lower limb and in postural control. For the VBM analysis, we considered the bilateral cortical motor regions [M1 foot area, supplementary motor area (SMA)], the bilateral cerebellar lobules VI and VIII, the bilateral cerebellar lobules IV and IX, the bilateral lobule V and the dentate nuclei. All these regions are involved in voluntary control of the limbs (Küper *et al.*, 2012). Regions involved in postural motor control included the medial vermis and the fastigial nuclei (Schmahmann *et al.*, 1999; Coffman *et al.*, 2011). The SMA, the cerebellar lobules, cerebellar vermis and deep cerebellar nuclei were extracted from wfupickatlas (<http://fmri.wfubmc.edu/software/PickAtlas>). The medial primary motor cortex was extracted from the Neurosynth atlas (<http://neurosynth.org/>; Yarkoni *et al.*, 2011). All these regions of interest were defined in the Montreal Neurological Institute (MNI) space. To define regions of interest in the thalamic nuclei, we considered the YeB atlas for subcortical structures (Yelnik *et al.*, 2007; Bardinat *et al.*, 2009). The ventro-lateral and ventral intermediate thalamic nuclei were automatically registered on the individual space of each participant's T_1 image. Thalamic nuclei were normalized in the MNI space using the transformation obtained from the VBM8 toolbox.

In the VBM analysis, we could not clearly separate the somatotopic representations in the cerebellar lobules. Thus, some additional precautions were taken for the resting state functional MRI analysis to test whether cerebellar functional abnormalities were specific to lower limbs somatotopic representation. The lateral cerebellar regions (lobules VI, VIII, IV, IX and V) were defined from the global maxima of clusters found in a previous study involving foot and hand movements (Küper *et al.*, 2012). Accordingly, the bilateral cerebellar lobules VI and VIII contained a mixed representation of the foot and hands, the bilateral cerebellar lobules IV and IX contained a representation of the foot specifically, the bilateral lobule V contained a representation of the hands. Regions of interest were defined as a sphere of 3 mm radius, centred on the global maxima obtained in the study of Kuper and collaborators (2012) (see Supplementary Table 1 for spatial coordinates).

In the resting state functional MRI analysis, in addition to the cerebello-thalamo-cortical network, we also studied a control network not directly involved in motor function i.e. the default mode network (DMN, e.g. Greicius *et al.*, 2004). This network included the bilateral medial prefrontal cortex, the

dorsolateral prefrontal cortex and the superior parietal cortex extracted from wfupickatlas.

Voxel-based morphometry

Images were processed with the VBM8 toolbox (<http://dbm.neuro.uni-jena.de/vbm/>), of SPM8 software (<http://www.fil.ion.ucl.ac.uk/spm/>) running under MATLAB R2010b (The MathWorks, Inc., Natick, MA). Normalized and modulated grey and white matter probability maps were obtained from T₁-weighted images. Processing included de-noising (Manjón *et al.*, 2010), partial volume estimation (Tohka *et al.*, 2004) and normalization to the MNI space using Dartel toolbox (Ashburner and Friston, 2005). The normalized maps were smoothed with a 10 mm filter-width at half-maximum (FWHM) Gaussian kernel.

The individual smoothed normalized grey matter maps were included in a two-sample *t*-test for group comparison. Age and gender were incorporated in the design matrix to remove the variance percentage related to variables of non-interest that could interfere with group differences. Individual values of intracranial volume were considered in the group model in the 'global calculation' option in the designation of the two-sample *t*-test in SPM8 to allow dealing with brain of different sizes.

Regression analysis was performed at the group level to test whether VBM individual measures within the whole brain (grey matter values) correlated with clinical measures (FAB score, duration of upright station, disease duration) and with EMG values quantifying tremor [amplitude (A) and width (w) of the EMG frequency peak]. We also sought correlations between individual VBM measures in the cerebellum and in the cortical motor areas. Age and gender were incorporated in the design matrix of the regression analysis to remove the variance percentage related to variables of non-interest that could interfere with the correlation.

Resting-state functional MRI analyses

Statistical parametric mapping software (SPM8, Wellcome Department of Cognitive Neurology, London, UK) was used for image processing (<http://www.fil.ion.ucl.ac.uk/spm/>). The functional images were interpolated in time to correct the time delay between slices (up to half the repetition time) during interleaved volume acquisition, and were realigned with the first image of each session. The anatomical image and the realigned functional images of each subject were normalized to a common standard space by using the MNI template. The functional data were spatially smoothed with an 8-mm FWHM Gaussian filter and temporally filtered with a 128 s period high-pass filter. Two types of analysis were performed: the first focused on the ALFF, and the second focused on functional connectivity within the cerebellar motor pathways. For each of these analyses, we look at possible correlation between ALFF or cerebellar functional connectivity with clinical/electrophysiological measures. Finally, we also looked at the modulation of cerebellar functional connectivity by the repetitive TMS procedure performed in a subsample of the orthostatic tremor patient population, and whether it correlated with the changes of clinical/electrophysiological measures.

In the first analysis, we modelled the amplitude of low-frequency fluctuations (ALFF) by using the procedures described in Song *et al.* (2011). A global linear model was defined for

each subject, and the contrast of interest was defined as the effect of the variance of the ALFF fluctuations in each subject. The resulting contrast maps were included in a two-sample *t*-test to identify changes of ALFF between the patients and the healthy volunteers in the regions of interest (see 'Regions of interest' section above).

Multiple regression analyses were used to identify correlations between ALFF in the regions of interest and clinical scores or electrophysiological variables.

In the second analysis, we performed a functional connectivity analysis of the cerebello-thalamo-cortical network, and of the default mode network. This analysis aimed at investigating functional connectivity of cerebellar structures showing abnormal grey matter volume and/or abnormal ALFF, taking these regions of interest as seeds to perform a whole brain analysis. Time series were extracted from the seed regions of interest (average signal of all the region of interest voxels) and entered as regressors in a global linear model in SPM8 (first level analysis), while regressing out the nuisance covariates individually (head movements, white matter and CSF signals). We run a group analysis using a two sample *t*-test to calculate group difference (between patients with orthostatic tremor and healthy volunteers) of cerebellar functional connectivity. Motor networks are bilateral in resting state studies. In addition, we did not expect an effect of hemisphere given that the tremor affects both body sides. Thus, the time series were extracted separately from right and left cerebellar structures, and were incorporated together in the group analysis, and further referred as bilateral cerebellar structures. The same procedure was performed for the right and left medial prefrontal cortices for the DMN.

Multiple regression analyses were used to identify correlations between functional connectivity in the networks of interest and clinical scores or electrophysiological variables.

Open label trial: effect of cerebellar repetitive transcranial magnetic stimulation on functional connectivity

The steps of image processing and the seed regions of the functional connectivity analysis were identical to the ones of the resting-state functional analysis of the main neuroimaging study. We ran an analysis using a paired *t*-test (patients with orthostatic tremor at baseline at Day 0, and patients with orthostatic tremor at Day 4) to calculate the modulation of the cerebellar network after five consecutive days of repetitive TMS applied on the cerebellum. The same procedure was performed to calculate the effect of the repetitive TMS treatment on the DMN (control network).

Regression analysis was performed at the group level to test whether cerebellar functional connectivity correlated with the potential improvement of clinical measures after five consecutive days of repetitive TMS (sFAB, duration of upright station) and with EMG values quantifying tremor (F, A and w) and recorded offline. The same procedure was performed for DMN.

Statistical threshold

Threshold of significance for two sample *t*-tests and multiple regression analyses was set at voxel-wise threshold of

$P < 0.001$ uncorrected at the level of the whole brain, with family-wise-error (FWE) correction at the level of the cluster, unless stipulated otherwise.

Results

Neuroimaging study

Clinical scores and electrophysiological measures of tremor

Age at disease onset and disease duration did not correlate with any clinical or EMG parameters ($-0.45 < r < 0.47$, $P > 0.05$). However, FAB scores correlated with the width of the tremor frequency peak ($Rho = -0.50$, $P < 0.05$) and the maximum duration of upright station ($Rho = 0.53$, $P < 0.05$). Thus, the multiple regression between grey matter volumes and each of the clinical parameters was evaluated taking into account the other related clinical parameters as covariates of non-interest (i.e. if the FAB was the clinical parameter of interest, the width of the tremor frequency peak and the duration of upright station were taken as co-variates of non-interest).

Voxel-based morphometry

Results and statistical values (F- or Z-scores) are shown in Fig. 1 and Table 2. Compared to the healthy volunteers, the whole-brain analysis showed that patients with orthostatic tremor had a bilateral decrease in the grey matter volume of cerebellar lobules VI. In the reverse contrast, the patients exhibited a bilateral increase in grey matter volume in the SMA proper predominating in the right hemisphere, and in the bilateral superior cerebellar vermis. There was no significant difference of grey matter volume in M1 foot/trunk area ($P > 0.09$).

The results of the multiple regression analysis are shown in Table 2. Grey matter volume in the cerebellar lobule VI correlated negatively with disease duration, and positively with the FAB score. In other words, greater atrophy levels in the cerebellar lobule VI were associated with longer disease duration and worse scores of postural instability (Fig. 2A). Though grey matter volume in the cerebellar lobule IX was not decreased, it correlated negatively with disease duration, and positively with the duration of the upright position. In other words, lower grey matter levels in the cerebellar lobule IX were associated with longer disease duration and ability to stand during a shorter period of time (Fig. 2B). The grey matter volume in the superior cerebellar vermis correlated positively with the duration of upright position (Table 2). In other words, greater increase of grey matter volume in the superior vermis was associated with the ability to stand during a longer period of time. Grey matter volume in the bilateral SMA proper correlated positively both with disease duration and with the surface (A) of the frequency peak: greater volumes were associated with longer disease duration and more severe tremor amplitude (Fig. 2C).

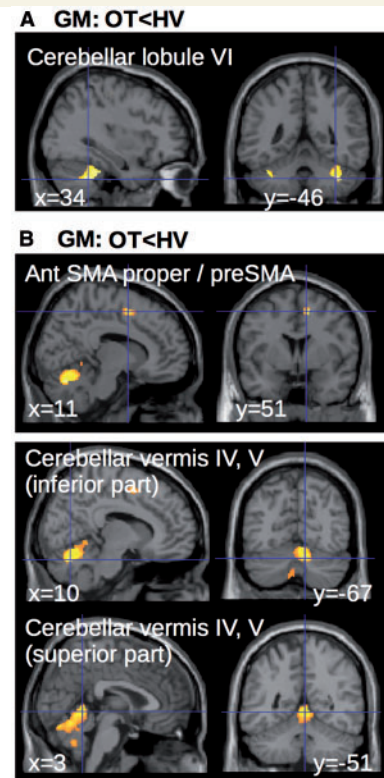


Figure 1 Group differences in voxel-based morphometry. Statistical parametric maps of the comparison between patients and healthy volunteers, showing (clusters are significant at $P < 0.05$, corrected for multiple comparisons at the cluster level) decreased grey matter (GM) volume in the cerebellum (A) and increased grey matter volume in both SMAs and superior cerebellar vermis (B). HV = healthy volunteer; OT = orthostatic tremor.

Scores at MMSE and SF36 questionnaire did not significantly correlate with grey matter volume in cerebellar motor pathways. See Supplementary material for correlations with other clinical scores.

Resting state functional MRI

Results of the first analysis showed that ALFF were higher in patients with orthostatic tremor compared to healthy volunteers bilaterally in the following areas: the posterior SMA proper, the preSMA, the superior part of the vermis (Fig. 3A) and the bilateral cerebellar lobules IX and IV (Fig. 3C). No difference was found in the reverse contrast. No significant difference was found between patients and healthy volunteers in the DMN. The regression analysis showed that higher ALFF in SMA proper and the superior cerebellar vermis (all regions where the grey matter was increased and the ALFF increased) were associated with higher tremor severity (higher 'A' values of the frequency peak) and longer durations of upright position maintained by the patients (Fig. 3B and Table 2).

Scores at MMSE and SF36 questionnaires did not significantly correlate with ALFF in cerebellar motor pathways. See Supplementary material for correlations with other clinical scores.

Table 2 Anatomical location of clusters displayed in Figs 1–3 with detailed statistics

Anatomical localization of clusters	Coordinates of global maxima [x y z]	Z-score	Ke
VBM grey matter changes			
OT > HV			
R Medial precentral gyrus (BA 6, preSMA, SMA proper)	15 3 62	3.78	157
R Vermis 7	8 -67 -26	3.43	2131
B Vermis 4,5	3 -51 -3	3.01	
OT < HV			
R Cerebellum, lateral lobule VI	34 -48 -39	3.22	677
L Cerebellum, lateral lobule VI	-38 -43 -33	3.06	66
Multiple regressions with grey matter			
Positive correlation with disease duration			
B Medial precentral gyrus (BA 6, preSMA, SMA proper)	-15 9 54	4.93	777
R Dentate nucleus	15 -66 -35	4.29	377
L Dentate nucleus	-12 -64 -36	3.96	213
Negative correlation with disease duration			
B Cerebellum, lateral lobule IX, vermis VIII and IX	8 -52 -54	5.63	1517
L Cerebellum, lateral lobule VI	-20 -61 -23	4.48	930
B Cerebellum, vermis VI	3 -75 -21	4.47	289
R Cerebellum lateral lobule VI	22 -58 -24	4.24	825
Positive correlation with FAB			
L Cerebellum, lateral lobule IV	-18 -36 -18	6.65	257
R Cerebellum, lateral lobule IV	8 -49 -2	5.34	82
L Cerebellum, lateral lobule VI	-33 -52 -35	3.77	83
Positive correlation with duration of SUR position			
R Cerebellum, lateral lobule IX	12 -48 -47	6.08	375
B Cerebellum, lobule IV, vermis III and IV	9 -46 -12	5.42	352
B Cerebellum, vermis VI	2 -67 -15	4.13	352
Positive correlation with EMG A			
B Medial precentral gyrus (BA 6, SMA proper)	3 0 55	3.19	172
ALFF changes			
OT > HV			
R Cerebellum, lateral lobule IX	9 -45 -48	4.14	327
L Cerebellum, lateral lobule IX	-10 -50 -39	3.77	448
R Medial precentral gyrus (BA 6, SMA proper)	16 -8 66	3.67	706
L Medial precentral gyrus (BA 6, SMA proper)	-6 -16 64	3.67	876
B Cerebellum, vermis III, IV, V	-3 -42 -9	3.66	907
Multiple regressions with ALFF			
Positive correlation with SUR duration			
R Medial precentral gyrus (BA 6, SMA proper)	12 -9 56	3.29	237
Positive correlation with EMG A			
R Medial precentral gyrus (BA 6, SMA proper)	12 -22 56	5.92	142
R Cerebellum, lobule IV and V	10 -54 -22	5.83	1497
L Cerebellum, lobule IV and V	-6 -52 -18	5.64	
B Cerebellum, vermis VIII	-3 -64 -40	5.70	146
L Paracentral lobule, foot area (BA 4)	-14 -36 -63	4.34	106

GM = grey matter; Bilat = bilateral; R = right; L = left; BA = Brodmann area; Ke = cluster volume (in number of voxels); OT = orthostatic tremor; HV = healthy volunteers; SUR = stand upright. Global maxima without cluster volume are included in the cluster above.

In the second analysis, three cerebellar regions of interest seeded the functional connectivity analysis: (i) the bilateral cerebellar lobule VI showing decreased grey matter volume, containing a mixed somatotopic representation of the hand and foot; (ii) the bilateral cerebellar lobule IX showing increased ALFF, containing a somatotopic representation of the foot; and (iii) the bilateral superior vermis showing an increase of grey matter volume and an increase of ALFF, involved in postural control of axial muscles. In this

section, we reported the results of regions of interest that were associated with motor manifestation of tremor. The ALFF in bilateral cerebellar lobule IX was correlated with the motor scores, but also with psychological scores evaluating the fear of falling. Therefore, functional connectivity results of this region of interest are presented in the Supplementary material. When comparing the patients with orthostatic tremor to the healthy volunteers, the cerebellar lobule VI had an increase of functional connectivity

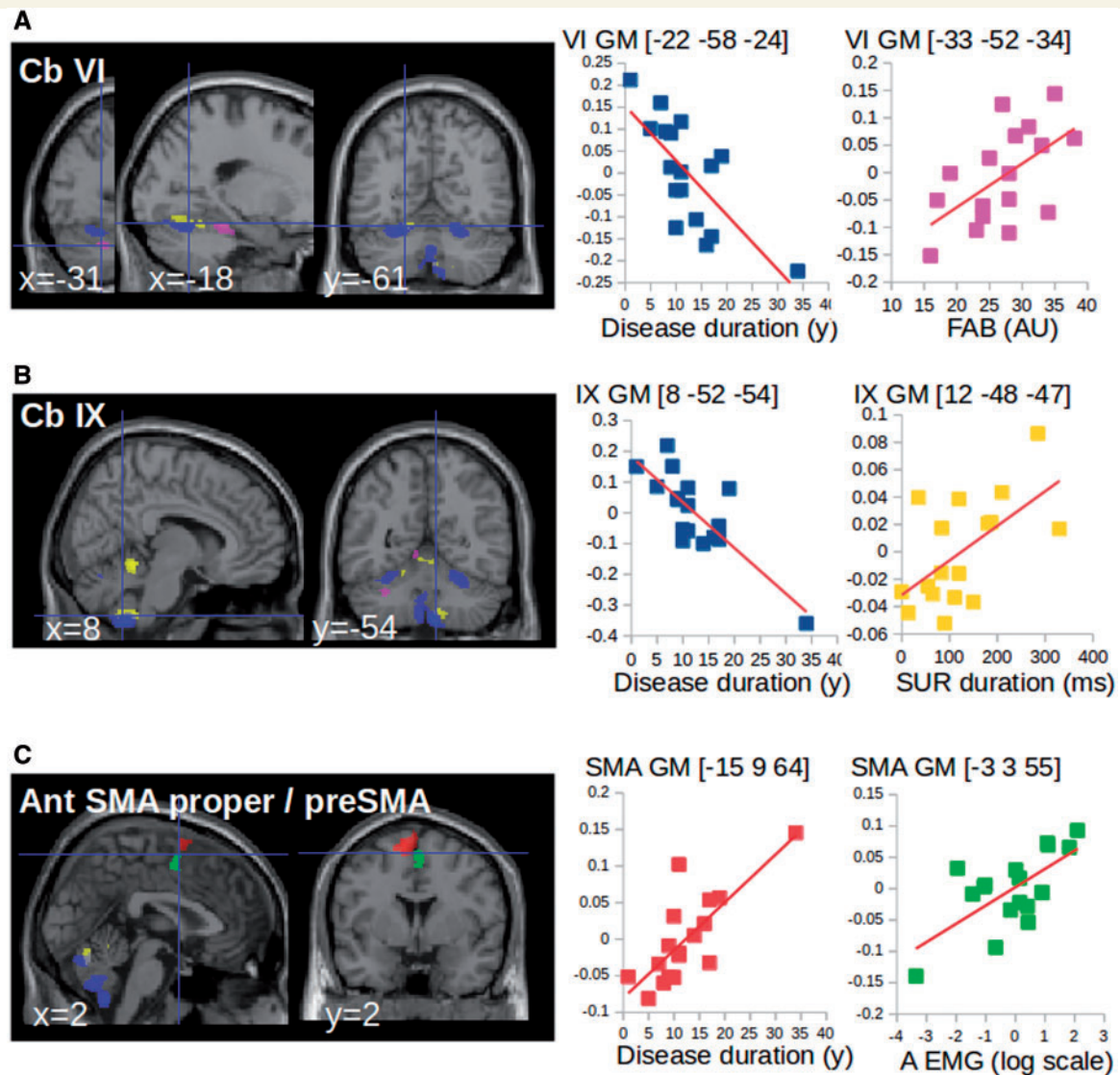


Figure 2 Correlation of VBM changes with clinical scores and tremor severity. (A and B) Multiple regression showing that grey matter volume in the cerebellum correlated negatively with disease duration (blue) and positively with clinical scores [SUR = stand upright station (yellow), FAB = Fullerton Assessment of Balance (magenta)]. (C) Multiple regression showing that grey matter volume in the SMA correlated positively with disease duration (red) and tremor characteristics (green). A = area of the tremor power spectrum measured from EMG recordings). The clusters are superimposed on the SPM canonical brain. The cerebral parameters (individual values) showing the correlations with clinical parameters were calculated voxel-by-voxel in the regions of interest of cerebello-thalamo-cortical network (see regions of interest definition). Graphics are used as a display to report data dispersion and the direction of the correlation. GM = grey matter.

with the bilateral SMA (Fig. 4A and C). Only the cerebellar lobule VI had an increase of functional connectivity with the M1 leg/trunk areas. Higher functional connectivity between the cerebellar lobule VI and the SMA proper was associated with more severe tremor as shown by the positive correlation found between the strength of the functional connectivity and the amplitude of the tremor frequency peak at baseline (Fig. 4B). We did not observe any difference between patients with orthostatic tremor and healthy volunteers regarding the functional connectivity between the superior vermis and the cortical motor areas. Details about the statistics and the anatomical localization of clusters are presented in Table 3.

Open label trial: effect of cerebellar repetitive transcranial magnetic stimulation on functional connectivity

Only one patient reported any subjective improvement of the tremor after 5 days of cerebellar stimulation. Accordingly the mean maximum duration that they could maintain an upright position was similar between baseline (107 ± 94.4 s), Day 5 (147 ± 143 s), Day 12 (113 ± 108 s) and Day 26 (137 ± 108 s) [repeated ANOVA: $F(3,24) = 1.8$, $P = 0.2$]. Also their postural instability was not improved [score on the FAB scale: 26 ± 4 at baseline,

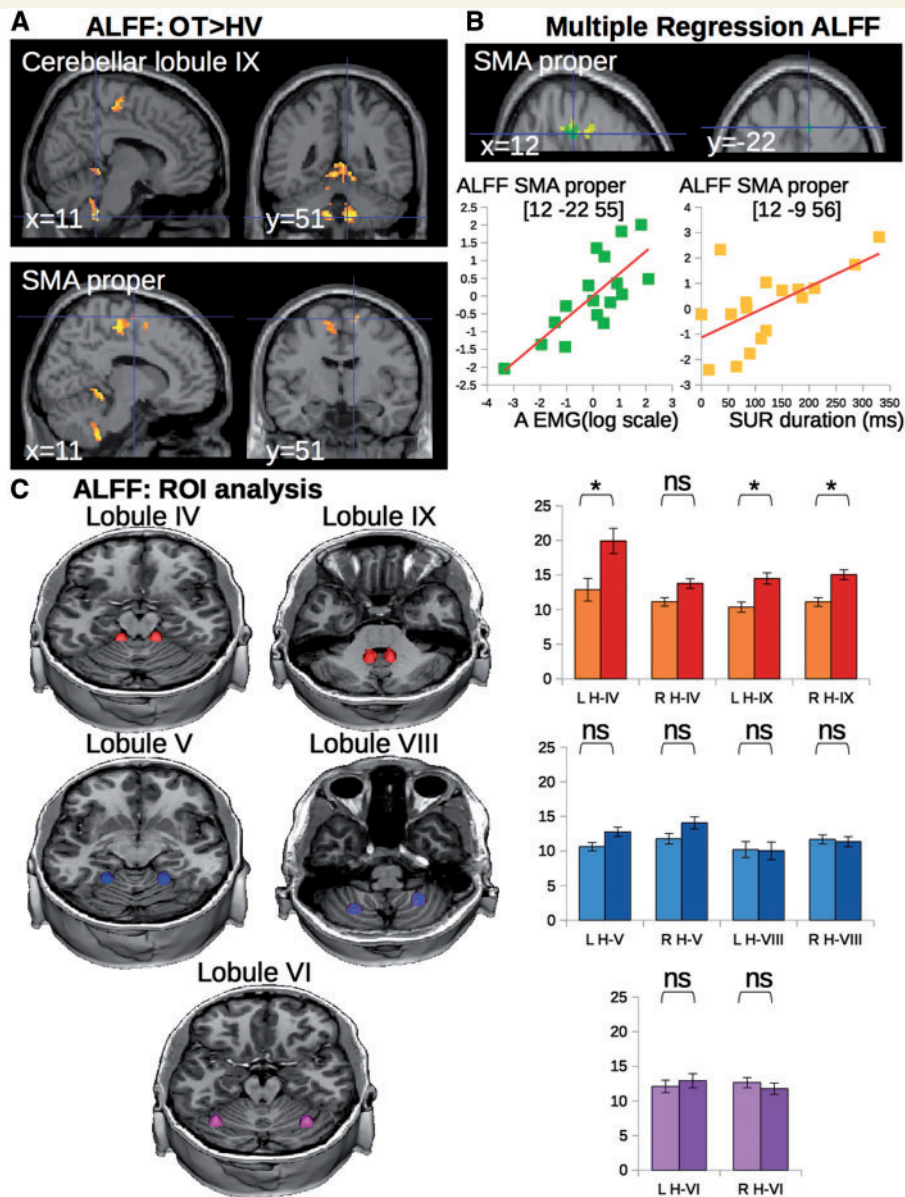


Figure 3 Group differences in ALFF and correlation of ALFF with clinical scores and tremor severity. (A) Statistical parametric maps showing the increase in ALFF in both SMA and superior cerebellar vermis of the patients with orthostatic tremor as compared with the healthy controls (clusters are significant at $P < 0.05$, corrected for multiple comparisons). (B) Multiple regression showing that ALFF in the SMA correlated with clinical scores (yellow) and tremor characteristics (green). Clusters are superimposed on the SPM canonical brain. Plots show the correlation between the global maximum in SMA (see Table 2 for statistical details and MNI coordinates). The cerebral parameters (individual values) showing the correlations with clinical parameters were calculated voxel-by-voxel in the regions of interest of cerebellar-motor circuit (see definition of regions of interest). (C) ALFF extracted from cerebellar clusters with lower and/or upper limb representation. Yellow–red = regions of lower limb representation (lobule IV and IX). Blue = regions of upper limb representation (lobule V and VIII). Purple = regions of complex representations of both lower and upper limbs (lobule VI). Graphs represent the average ALFF in each group (light = healthy volunteers, dark = patients with orthostatic tremor). Asterisks represent a significant group difference at $P < 0.05$ corrected for multiple comparisons. NS = non-significant; LH = left hemisphere; RH = right hemisphere; IV = cerebellar lobule IV; V = cerebellar lobule V; VI = cerebellar lobule VI; VIII = cerebellar lobule VIII; IX = cerebellar lobule IX; OT = orthostatic tremor; ROI = region of interest; SUR = stand upright station.

28 ± 6 at Day 5, 29 ± 5 at Day 12, 29 ± 8 at Day 26; repeated ANOVA: $F(3,24) = 1.5$, $P = 0.2$] (Fig. 5A).

Contrasting with the lack of clinical improvement the amplitude of the tremor was significantly reduced as shown by the decrease of the surface ('A') of the peak of

the tremor power spectrum [baseline: 3.8 ± 3.2 (m/s^2)², Day 5: 2.4 ± 2.2 (m/s^2)², Day 12: 1.9 – 3.1 (m/s^2)², Day 26: 1.5 ± 1.6 (m/s^2)²; repeated ANOVA: $F(3,24) = 3.1$, $P < 0.04$; *post hoc* Bonferroni test: Day 1 versus Day 26, $P < 0.006$] (Fig. 5A).

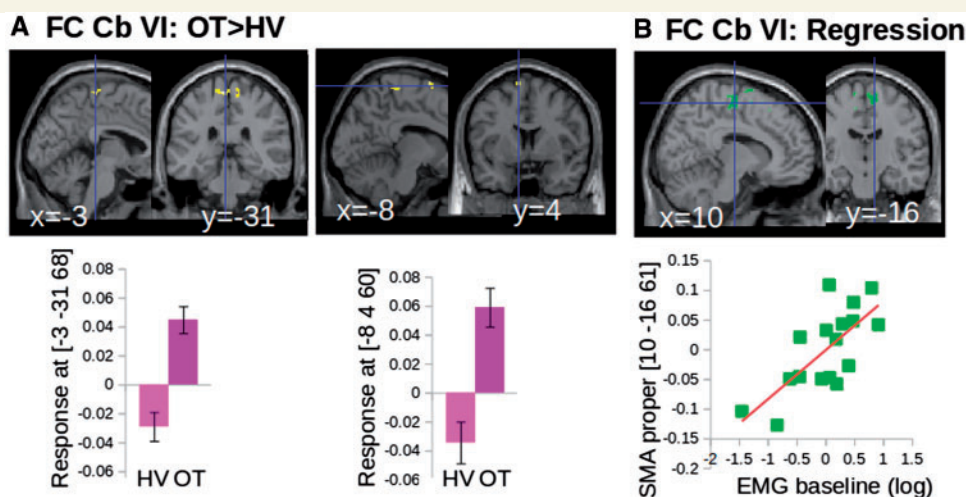


Figure 4 Results of functional connectivity of cerebellar motor networks. (A) Increased functional connectivity between the cerebellar lobule VI and both the lower limb representation of M1 and the SMA in patients with orthostatic tremor (OT) compared to healthy volunteers (HV) displayed on the SPM canonical brain (top) and represented graphically (bottom). (B) Multiple regression results showing that functional connectivity between the cerebellum VI and the SMA correlated with tremor characteristics on the SPM canonical brain (top) and represented graphically (bottom). All group differences and multiple regression results are significant at $P < 0.05$ corrected at the level of the cluster. Clusters are superimposed on the SPM canonical brain. Plots display the dispersion of data points extracted from the global maximum (see Table 3 for statistical details).

After 5 days of cerebellar stimulation, the bilateral cerebellar lobule VI had a decreased of functional connectivity with both the SMA and the M1 leg/trunk area compared to baseline (Fig. 5B and Table 3). There was no functional connectivity change between the superior vermis and the cortical motor areas. Before cerebellar repetitive TMS, higher functional connectivity between the cerebellar lobule VI and the SMA proper was associated with more severe tremor in the nine patients participating in the open label trial (Fig. 5C), similarly to the results obtained on the whole population (Fig. 4C). At Day 5, cerebellar stimulation cancelled the relationship between functional connectivity of the cerebello-cortical network and the surface 'A' of the peak of the tremor power spectrum (Fig. 5C, graph on the middle panel). When looking at prolonged behavioural effects, functional connectivity between the cerebellar lobules VI and the SMA proper after 5 days of cerebellar stimulation predicted the decrease of the surface 'A' of the peak of the tremor power spectrum at day 26 (Fig. 5C, graph of the right panel). In this case, lower functional connectivity between the cerebellar lobule VI and SMA proper was associated with more severe tremor. Functional connectivity of cerebellar lobule IX did not correlate with the surface 'A' of the peak of the tremor power spectrum at Day 26. Details about the statistics and the anatomical localization of clusters are presented in Table 3.

After 5 days of cerebellar stimulation, the bilateral medial prefrontal cortex had equal level of functional connectivity with both the bilateral dorsolateral prefrontal cortex and the bilateral superior parietal cortex compared to baseline. The multiple regression analysis did not show any correlation between functional connectivity of the DMN at Day

5 and the amplitude of the tremor frequency peak at Day 5 or Day 26.

Discussion

This study highlights (i) the involvement of the lateral posterior cerebellum (lobule VI) in the core pathological process of orthostatic tremor; (ii) the contribution of its output pathways to the premotor and motor cortices in the postural imbalance of patients with orthostatic tremor; and (iii) the compensatory role of the cerebellar vermis. The present findings shed a new light on the structural defects and intrinsic functional substrates of unsteadiness and imbalance in orthostatic tremor.

The patients with orthostatic tremor exhibited cerebellar atrophy, as revealed by lower grey matter volumes in bilateral lobule VI. In the whole brain analysis, no other subcortical or cortical zone exhibited decreased grey matter volume in patients compared to controls. The fact that greater atrophy levels in cerebellar lobule VI were associated with longer disease duration and worse scores of postural instability (Fig. 2A) highlights the functional significance of these structural changes and associate them with the core disorder. Though the grey matter volume was not decreased in bilateral lobule IX in the group comparison, it is likely that lobule IX impairment is also part of the core disorder because lower grey matter volume in lobule IX was associated with longer disease duration and more severe unsteadiness (Fig. 2B). It is worth noting that functional changes in cerebellar lobule IX were also associated with non-motor manifestations (scores at COF measuring psychological consequences of the fear of falling)

Table 3 Anatomical location of clusters displayed in Figs 4–5 with detailed statistics

Anatomical localization of clusters		Coordinates of global maxima [x y z]	Z-score	Ke
Functional connectivity at baseline (Fig. 4)				
FC cerebellum Lobule VI (Fig. 4A)				
OT > HV				
L	Medial precentral gyrus, paracentral lobule (BA 4,3,1, M1 foot area)	−4 −32 68	5.40	160
R	Medial precentral gyrus, paracentral lobule (BA 4,3,1, M1 foot area)	4 −22 69	4.30	
R	Medial precentral gyrus (BA 6, SMA proper)	12 −4 72	5.29	25
L	Medial precentral gyrus (BA 6, preSMA)	−10 6 72	4.77	43
Multiple regressions with FC cerebellum lobule VI (Fig. 4B)				
Positive correlation with EMG A at Day 1				
L	Medial precentral gyrus (BA 6, preSMA)	−6 20 58	5.88	106
L	Medial precentral gyrus (BA 6, SMA proper)	−10 −14 68	5.66	93
R	Medial precentral gyrus (BA 6, SMA proper)	10 −16 62	5.65	258
Open label trial: effect of rTMS on functional connectivity (Fig. 5)				
FC cerebellum lobule VI (Fig 5B)				
Baseline > rTMS				
R	Paracentral lobule, medial postcentral gyrus (BA 3,2,1), medial precentral gyrus (BA 4, M1 foot area)	2 −44 62	8.11	1316
R	Precentral gyrus (BA 6, SMA proper)	12 −8 72	6.93	
B	Medial precentral gyrus (BA 6, SMA proper)	0 −0 57	6.91	
L	Precentral gyrus (BA 4, M1 foot area)	−14 −33 70	6.62	82
Multiple regressions with FC cerebellum lobule VI (Fig 5C)				
Positive correlation with EMG A (Day 5)				
L	Precentral/postcentral gyrus (BA 4,3, M1 foot area)	−16 −34 69	7.21	46
R	Medial precentral gyrus (BA 6, SMA proper)	14 −20 54	6.20	39
R	Precentral/postcentral gyrus (BA 4,3, M1 foot area)	6 −42 68	5.99	147
L	Medial precentral gyrus (BA 6, SMA proper)	−9 −8 56	5.30	60
Positive correlation with EMG A (Day 26)				
R	Medial precentral gyrus (BA 6, SMA proper)	14 −6 52	16.35	49
L	Medial precentral gyrus (BA 6, SMA proper)	−12 −4 64	10.63	375
L	Medial precentral gyrus (BA 6, SMA proper)	−3 −4 50	7.98	75
R	Precentral/postcentral gyrus (BA 4,3, M1 foot area)	6 −26 74	7.54	38

Bilat = bilateral, R = right, L = left, BA = Brodmann area. Ke = cluster volume (number of voxels); FC = functional connectivity; rTMS = repetitive TMS; OT = orthostatic tremor; HV = healthy volunteers. Global maxima without cluster volume are included in the cluster above.

of orthostatic tremor (Supplementary Fig. 1). It is possible that functional changes seen in this area may be related to the tremor effect on posture and gait.

Another feature of orthostatic tremor, in addition to the cerebellar atrophy, was an increased grey matter volume of the preSMA and SMA proper, which was accompanied by increased amplitude of low frequency fluctuation of the BOLD signal. The SMA plays an important role in postural balance control; for example a positive correlation was found between the postural task-related SMA activity and individual balance ability in stroke patients (Mihara *et al.*, 2012). The SMA is thought to contribute to the modulation of anticipatory postural adjustments (Bolzoni *et al.*, 2015) leading to step initiation. Both SMA activation and step initiation are impaired in Parkinson's disease with freezing of gait (Fling *et al.*, 2014). Premotor areas including the SMA are a well-documented target of the cerebellum lobule VI, which is part of the sensorimotor cerebello-cerebral network (Habas, 2010; O'Reilly *et al.*, 2010; Buckner *et al.*, 2011). The SMA could receive constant erroneous messages due to an impaired processing of the lower limb proprioceptive afferents in the cerebellar lobules IV, VI and

IX. This would result in the strong feeling of unsteadiness in the patients with orthostatic tremor and their impaired ability to maintain the standing position. Results from an EEG-EMG coherence study in patients with orthostatic tremor strongly support this hypothesis (Muthuraman *et al.*, 2013). In this EEG study, cerebellar and SMA sources were among the areas of the network oscillating at orthostatic tremor frequency. The authors propose that changes of cortico-muscular coherence are linked in some way to desynchronization of lower limbs proprioceptive feedback causing an increase of unsteadiness. In our study, functional MRI signal was recorded in absence of tremor, preventing us from assessing the direct relationship between brain activation and tremor-related oscillations.

Our results of functional connectivity within the cerebellar sensorimotor networks confirmed the functional relevance of the communication between the bilateral cerebellar lobules and the SMA to the orthostatic tremor pathology. Indeed, patients had increased functional connectivity between cerebellar lobule VI and both the SMA and the lower limb representation of the primary motor cortices, when compared to controls. In addition, the

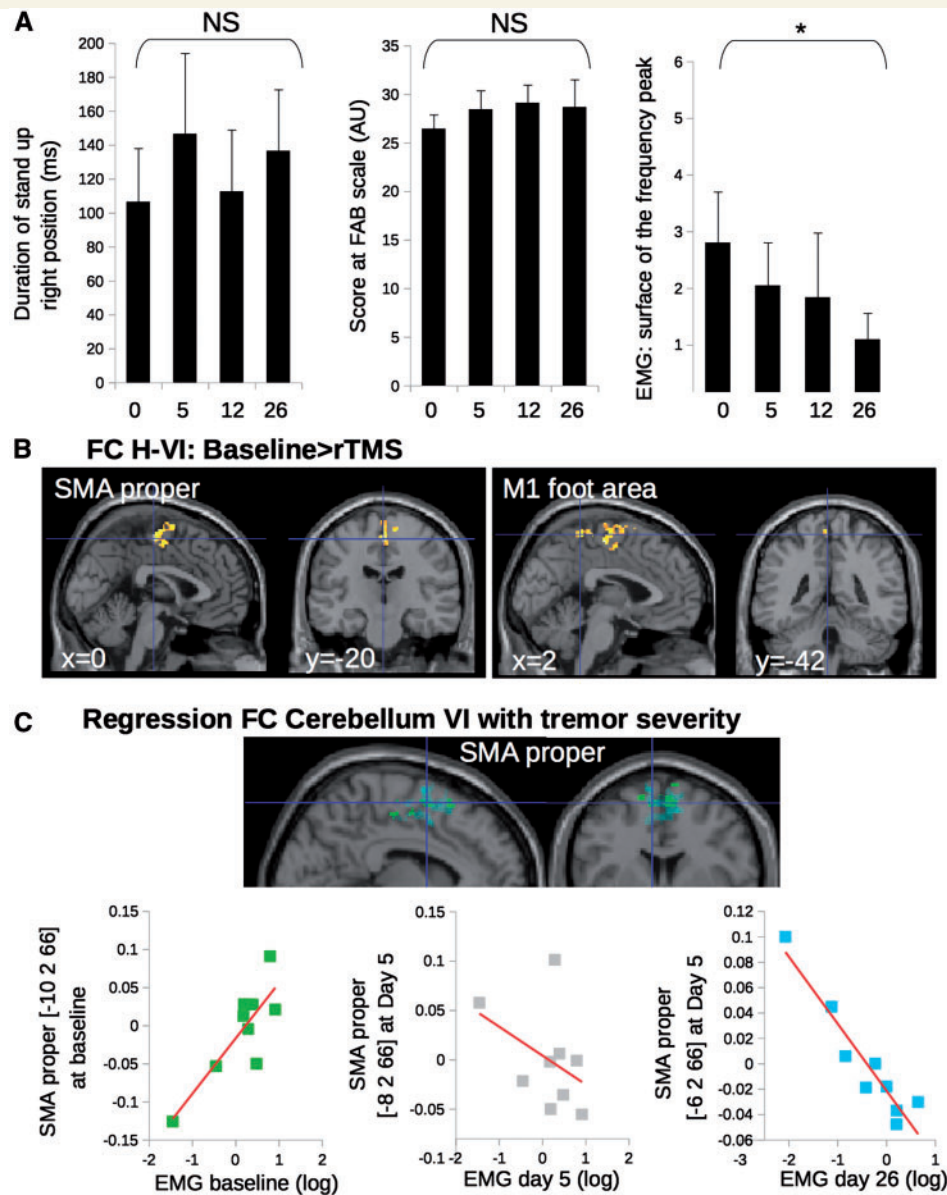


Figure 5 Results of functional connectivity of cerebellar motor networks for the open label trial with repetitive TMS of the cerebellum. (A) Effect of repetitive TMS on the clinical and electrophysiological characteristics of tremor. Asterisks represent a significant effect of repetitive TMS between Day 26 and baseline. (B) Compared to baseline, patients with orthostatic tremor had a decrease of functional connectivity (FC) after repetitive TMS (rTMS) treatment between the bilateral cerebellar lobule VI and both the lower limb representation in M1 and the SMA. Group differences are significant at $P < 0.05$ corrected at the level of the cluster. (C) Multiple regression showing that functional connectivity between the cerebellum VI and the SMA correlated with tremor characteristics positively at baseline (green) but negatively at Day 26 (cyan). This correlation was not significant at Day 5 (grey). Clusters are superimposed on the SPM canonical brain. Plots show the data dispersion and the direction of the correlation (see Table 3 for statistical details and MNI coordinates).

connectivity within the cerebellar lobules VI-SMA network correlates with the amplitude of the tremor frequency peak quantified from the EMG at baseline (Fig. 4): higher level of functional connectivity was associated with higher amplitude of the tremor frequency peak. This suggests that cerebellar structural changes may have cascading effects on the functional involvement of the output pathways from these lobules to the motor (lower limb) and the SMA.

The results of the repetitive TMS trial support the functional relevance of cerebello-cerebral connections involving the SMA for orthostatic tremor. However, controlled studies are needed to rule out a possible placebo effect. After five consecutive days of cerebellar 1 Hz repetitive TMS, the amplitude of the EMG frequency peak reflecting the tremor severity was reduced. In addition, the relationship between functional connectivity between lobule VI-SMA and the

amplitude of the EMG frequency peak is reversed. The stimulation could modulate the cerebellar processing of the lower limb proprioceptive afferences and decrease the amount of erroneous messages exchanged with the SMA. This suggests that functional engagement of cerebellar motor pathways involving the SMA is less needed when tremor is reduced. The stimulation induced specific changes of the lateral cerebello-cortical connectivity yet no change in the medial cerebello-cortical connectivity involving the vermis, nor in the DMN.

A similar pattern of structural changes in the lateral cerebellum and the SMA was observed in essential tremor. Cerebellar atrophy is often found in essential tremor (see review by Cerasa and Quattrone, 2016), and was recently associated with changes of grey matter volume in SMA (Gallea *et al.*, 2015). SMA abnormal functioning in essential tremor has also been shown using functional MRI (Gallea *et al.*, 2015; Broersma *et al.*, 2016; Yin *et al.*, 2016). In orthostatic tremor, brain structural analysis is missing so far and the few functional data indicate hyperactivity of the SMA (Wills *et al.*, 1996; Guridi *et al.*, 2008). When all the results are put together with our study, cerebellar atrophy and an increase of ALFF in the SMA were commonly found in orthostatic tremor, as in essential tremor. This pattern could represent common morphological changes as a generic intrinsic signature of certain types of tremors. If so, how do we explain that the tremor affects different body parts at different frequencies in essential tremor and orthostatic tremor? One explanation for the involvement of different body parts would be that the pathological process affects different parts of the cerebellar motor homunculus somatotopy. A complex motor somatotopy was described in the human cerebellum by means of functional MRI (Grodz *et al.*, 2001; Schlerf *et al.*, 2010; Küper *et al.*, 2012). Movement-related activations revealed a somatomotor representation in the anterior lobe with the foot representation more anterior and medial (possibly in lobule IV) than the hand representation (possibly in lobule V) [see Figure 5 in Schlerf *et al.* (2010); and Figure 5 in Küper *et al.* (2012)]. Another somatomotor representation was found in the posterior cerebellum with hand movements more in lobule VIII and foot movements more in lobule IX (Küper *et al.*, 2012). Schlerf and colleagues (2010) described a third somatomotor representation in lobule VI that would support complex movements and has symmetric motor representations of arms and legs in both hemispheres, with the leg representation more lateral. In keeping with this view, patients with orthostatic tremor had impairments predominantly in those cerebellar zones containing lower limb representations (atrophy in the lateral lobule VI and increased ALFF in lobules IX and IV) while essential tremor patients previously studied (Gallea *et al.*, 2015) had more impairment in the lobules V and VIII.

Another important finding of the present study was the increase of grey matter volume in the cerebellar vermis, which seems to be specific to orthostatic tremor pathology,

not being found in patients with essential tremor (Passamonti *et al.*, 2012; Gallea *et al.*, 2015). Larger grey matter volume in the vermis was associated with longer disease duration and better ability to keep a standing position. Taken together, these correlations are suggestive of compensatory mechanisms that might develop in the vermis over the evolution of the disease. The functional implication of the vermis in orthostatic tremor was only reported in one single-case PET study, describing vermis hypermetabolism in a patient with 16 Hz orthostatic tremor (Wills *et al.*, 1996). A potential compensatory role was not suggested.

We speculate that the lower limbs tremor that causes a strong postural impairment could trigger compensatory mechanisms in the vermis through brainstem nuclei and the descending pathways to the spinal cord, as this structure is known to play a major role in posture. It has recently been shown from monkey studies, that the superior cerebellar vermis is a major target of projections from the cerebral cortex (primary motor cortex, SMA) and that these projections could be part of the neural substrate for anticipatory postural adjustments (Coffman *et al.*, 2011). The major output of the vermis is to the fastigial nucleus, which encodes proprioceptive inputs during body motion (Brooks and Cullen, 2009). Twenty-five per cent of the projections of the fastigial nucleus target the ventral intermediate nucleus of the thalamus, while the remaining projections target the descending pathways to the brainstem and the spinal cord (Asanuma *et al.*, 1983; Coffman *et al.*, 2011). The major output from the fastigial nucleus participates in the control of whole body posture, orientation and locomotion. This is in agreement with our functional connectivity results showing no group difference in the communication between the superior vermis, the thalamus and the motor cortical areas. In our patients the verminal hypertrophy was found in the superior vermis and not in the caudal vestibular part of the vermis (IX–X), suggesting that the vestibular cerebellum might not be involved in orthostatic tremor. Moreover, the stimulation of the cerebellar hemisphere decreased the tremor amplitude but did not impact the functional connectivity between the vermis and the premotor area. This further supports that the vermis-induced compensatory effect is likely exerted through the descending verminal projections to the spinal cord.

Potential limitations

The engagement of the cerebello-thalamo-cortical in our patients with orthostatic tremor was recorded in the absence of tremor itself. MRI recordings were acquired on patients in supine position when they were free of any tremor. Thus, our results cannot be interpreted in terms of tremor generation, but as subjacent changes associated with this pathology. Nevertheless, some of our results are consistent with the results of PET studies in which brain activation was recorded in concomitance with tremor. A single case study involving an orthostatic tremor patient

during upright standing showed hypermetabolism in the primary motor cortex and the cerebellar vermis (Guridi *et al.*, 2008). Another study involving four patients with orthostatic tremor in supine position with their outstretched right upper limb causing a 14–16 Hz arm tremor, found hypermetabolism bilaterally in the cerebellar hemispheres, the cerebellar vermis, and in the thalamus (Wills *et al.*, 1996). Thus, the present resting state study was successful in isolating brain networks that show intrinsic abnormalities that are also observed during tremor occurrence. Any parameter extracted from functional MRI data is by its nature indirectly linked to any macroscopic manifestation of a (patho)physiological process.

Due to limited temporal resolution of functional MRI, our study could not provide any information about any possible high frequency oscillatory activity related to the 14–18 Hz tremor travelling within the cerebello-thalamo-cortical network in orthostatic tremor. Future studies using EEG and/or MEG with higher temporal resolution during the occurrence of tremor could investigate the coherence between the EMG and the activation of the nodes of the cerebello-thalamo-cortical network.

Among the 17 patients involved in the study, 11 patients had clonazepam medication. Individual clonazepam intake was considered as a nuisance covariable in all the analyses. Blood monitoring of the unbound clonazepam levels would have helped in removing more precisely the effect of the medication on the ALFF and the functional connectivity analyses. However this procedure was not included in the Institutional Review Board-approved protocol.

As we did perform a resting-activation study, we could not superpose directly the somatomotor representations of the lower limbs on the areas with structural or functional defects. Our suggestion that different body part representations are involved in essential tremor and orthostatic tremor is based on *a priori* somatotopic regions taken from atlases or other studies looking at lower limb representation. However, patients with orthostatic tremor could have abnormal representation of the lower limb, which we did not specifically measure in the present study.

As our repetitive TMS design did not include sham stimulation, we cannot completely rule out a placebo effect. However, such a placebo effect is unlikely, as the stimulation did not induce any subjective improvement; the decrease of tremor amplitude was only noticeable on the EMG analysis. Also, the stimulation induced specific changes of the lateral cerebello-cortical connectivity and no change in the medial cerebello-cortical connectivity involving the vermis, nor in the default mode network.

Acknowledgements

We thank the Center for Clinical Investigations (CIC) Pitié-Salpêtrière N° 9503 and the platform ‘CENIR–PANAM:

physiology and analysis of movement core facility’ of CR-ICM for their invaluable support with the experiments.

Funding

This research was conducted within the framework of the APHP ‘Assistance publique Hopitaux de Paris #C10-01. This work received financial support from the patient associations ‘Association des Personnes concernées par le Tremblement Essentiel’ (APTES) and the ‘National Organization for Rare Disorders’ (NORD), Fondation pour la Recherche Médicale (programme ‘Espoir de la recherche’, ‘Postdoctorat en France’ grant attributed to CG), Contrats d’interface INSERM/APHP (SM) and interface CNRS/APHP (ER), Investissements d’avenir ANR-10-IAIHU-06 (Paris Institute of Neurosciences – IHU).

Supplementary material

Supplementary material is available at *Brain* online.

References

- Asanuma C, Thach WT, Jones EG. Distribution of cerebellar terminations and their relation to other afferent terminations in the ventral lateral thalamic region of the monkey. *Brain Res* 1983; 286: 237–65.
- Ashburner J, Friston KJ. Unified segmentation. *Neuroimage* 2005; 26: 839–51.
- Bardinet E, Bhattacharjee M, Dormont D, Pidoux B, Malandain G, Schüpbach M, et al. A three-dimensional histological atlas of the human basal ganglia. II. Atlas deformation strategy and evaluation in deep brain stimulation for Parkinson disease. *J Neurosurg* 2009; 110: 208–19.
- Benito-León J, Rodríguez J, Ortí-Pareja M, Ayuso-Peralta L, Jiménez-Jiménez FJ, Molina JA. Symptomatic orthostatic tremor in pontine lesions. *Neurology* 1997; 49: 1439–41.
- Biswal B, Yetkin FZ, Haughton VM, Hyde JS. Functional connectivity in the motor cortex of resting human brain using echo-planar MRI. *Magn Reson Med* 1995; 34: 537–41.
- Bolzoni F, Bruttini C, Esposti R, Castellani C, Cavallari P. Transcranial direct current stimulation of SMA modulates anticipatory postural adjustments without affecting the primary movement. *Behav Brain Res* 2015; 291: 407–13.
- Broersma M, van der Stouwe AMM, Buijink AWG, de Jong BM, Groot PFC, Speelman JD, et al. Bilateral cerebellar activation in unilaterally challenged essential tremor. *Neuroimage Clin* 2016; 11: 1–9.
- Brooks JX, Cullen KE. Multimodal integration in rostral fastigial nucleus provides an estimate of body movement. *J Neurosci* 2009; 29: 10499–511.
- Buckner RL, Krienen FM, Castellanos A, Diaz JC, Yeo BTT. The organization of the human cerebellum estimated by intrinsic functional connectivity. *J Neurophysiol* 2011; 106: 2322–45.
- Cerasa A, Quattrone A. Linking essential tremor to the cerebellum—neuroimaging evidence. *Cerebellum* 2016; 15: 263–75. DOI :10.1007/s12311-015-0739-8.

- Coffman KA, Dum RP, Strick PL. Cerebellar vermis is a target of projections from the motor areas in the cerebral cortex. *Proc Natl Acad Sci USA* 2011; 108: 16068–73.
- Contarino MF, Bour LJ, Schuurman PR, Blok ER, Odekerken VJJ, van den Munckhof P, et al. Thalamic deep brain stimulation for orthostatic tremor: clinical and neurophysiological correlates. *Parkinsonism Relat Disord* 2015; 21: 1005–7.
- Deuschl G, Bain P, Brin M. Consensus statement of the movement disorder society on tremor. *Ad Hoc Scientific Committee. Mov Disord* 1998; 13 (Suppl 3): 2–23.
- Espay AJ, Duker AP, Chen R, Okun MS, Barrett ET, Devoto J, et al. Deep brain stimulation of the ventral intermediate nucleus of the thalamus in medically refractory orthostatic tremor: preliminary observations. *Mov Disord* 2008; 23: 2357–62.
- Feil K, Böttcher N, Guri F, Krafczyk S, Schöberl F, Zwergal A, et al. Long-term course of orthostatic tremor in serial posturographic measurement. *Parkinsonism Relat Disord* 2015; 21: 905–10.
- Fling BW, Cohen RG, Mancini M, Carpenter SD, Fair DA, Nutt JG, et al. Functional reorganization of the locomotor network in Parkinson patients with freezing of gait. *PLoS One* 2014; 9: e100291.
- Fung VS, Sauner D, Day BL. A dissociation between subjective and objective unsteadiness in primary orthostatic tremor. *Brain J Neurol* 2001; 124: 322–30.
- Gallea C, Popa T, García-Lorenzo D, Valabregue R, Legrand A-P, Marais L, et al. Intrinsic signature of essential tremor in the cerebello-frontal network. *Brain J Neurol* 2015; 138: 2920–33.
- Ganos C, Maugest L, Apartis E, Gasca-Salas C, Cáceres-Redondo MT, Erro R, et al. The long-term outcome of orthostatic tremor. *J Neurol Neurosurg Psychiatry* 2016; 87: 167–72.
- Gerschlagler W, Münchau A, Katzenschlager R, Brown P, Rothwell JC, Quinn N, et al. Natural history and syndromic associations of orthostatic tremor: a review of 41 patients. *Mov Disord* 2004; 19: 788–95.
- Greicius MD, Srivastava G, Reiss AL, Menon V. Default-mode network activity distinguishes Alzheimer's disease from healthy aging: evidence from functional MRI. *Proc Natl Acad Sci USA* 2004; 101: 4637–42.
- Grodd W, Hülsmann E, Lotze M, Wildgruber D, Erb M. Sensorimotor mapping of the human cerebellum: fMRI evidence of somatotopic organization. *Hum Brain Mapp* 2001; 13: 55–73.
- Guridi J, Rodriguez-Oroz MC, Arbizu J, Alegre M, Prieto E, Landecheo I, et al. Successful thalamic deep brain stimulation for orthostatic tremor. *Mov Disord* 2008; 23: 1808–11.
- Habas C. Functional imaging of the deep cerebellar nuclei: a review. *Cerebellum Lond Engl* 2010; 9: 22–8.
- Kızıltan ME, Gündüz A, Kızıltan G, Sayılır I, Benbir G, Uyanık O. Acoustic startle response in patients with orthostatic tremor. *Neurosci Lett* 2012; 525: 100–4.
- Küper M, Thürling M, Stefanescu R, Maderwald S, Roths J, Elles HG, et al. Evidence for a motor somatotopy in the cerebellar dentate nucleus—an fMRI study in humans. *Hum Brain Mapp* 2012; 33: 2741–9.
- Lyons MK, Behbahani M, Boucher OK, Caviness JN, Evidente VGH. Orthostatic tremor responds to bilateral thalamic deep brain stimulation. *Tremor Hyperkinetic Mov* 2012; 2: tre-02-30-85-9.
- Magariños-Ascone C, Ruiz FM, Millán AS, Montes E, Regidor I, del Alamo de Pedro M, et al. Electrophysiological evaluation of thalamic DBS for orthostatic tremor. *Mov Disord* 2010; 25: 2476–7.
- Manjón JV, Tohka J, Robles M. Improved estimates of partial volume coefficients from noisy brain MRI using spatial context. *Neuroimage* 2010; 53: 480–90.
- Mestre TA, Lang AE, Lang AE, Ferreira JJ, Almeida V, de Carvalho M, et al. Associated movement disorders in orthostatic tremor. *J Neurol Neurosurg Psychiatry* 2012; 83: 725–9.
- Mihara M, Miyai I, Hattori N, Hatakenaka M, Yagura H, Kawano T, et al. Cortical control of postural balance in patients with hemiplegic stroke. *Neuroreport* 2012; 23: 314–19.
- Muthuraman M, Hellriegel H, Paschen S, Hofschulte F, Reese R, Volkmann J, et al. The central oscillatory network of orthostatic tremor. *Mov Disord* 2013; 28: 1424–30.
- Norton JA, Wood DE, Day BL. Is the spinal cord the generator of 16-Hz orthostatic tremor? *Neurology* 2004; 62: 632–34.
- O'Reilly JX, Beckmann CF, Tomassini V, Ramnani N, Johansen-Berg H. Distinct and overlapping functional zones in the cerebellum defined by resting state functional connectivity. *Cereb Cortex* 2010; 20: 953–65.
- Passamonti L, Cerasa A, Quattrone A. Neuroimaging of essential tremor: what is the evidence for cerebellar involvement? *Tremor Hyperkinetic Mov* 2012; 2.
- Piboolnurak P, Yu QP, Pullman SL. Clinical and neurophysiologic spectrum of orthostatic tremor: case series of 26 subjects. *Mov Disord* 2005; 20: 1455–61.
- Popa T, Russo M, Vidailhet M, Roze E, Lehericy S, Bonnet C, et al. Cerebellar rTMS stimulation may induce prolonged clinical benefits in essential tremor, and subjacent changes in functional connectivity: an open label trial. *Brain Stimulat* 2013; 6: 175–9.
- Rose DJ, Lucchese N, Wiersma LD. Development of a multidimensional balance scale for use with functionally independent older adults. *Arch Phys Med Rehabil* 2006; 87: 1478–85.
- Schlerf JE, Verstynen TD, Ivry RB, Spencer RMC. Evidence of a novel somatotopic map in the human neocerebellum during complex actions. *J Neurophysiol* 2010; 103: 3330–6.
- Schmahmann JD, Doyon J, McDonald D, Holmes C, Lavoie K, Hurwitz AS, et al. Three-dimensional MRI atlas of the human cerebellum in proportional stereotaxic space. *Neuroimage* 1999; 10: 233–60.
- Schnitzler A, Münks C, Butz M, Timmermann L, Gross J. Synchronized brain network associated with essential tremor as revealed by magnetoencephalography. *Mov Disord* 2009; 24: 1629–35.
- Setta F, Jacquy J, Hildebrand J, Manto MU. Orthostatic tremor associated with cerebellar ataxia. *J Neurol* 1998; 245: 299–302.
- Setta F, Manto MU. Orthostatic tremor associated with a pontine lesion or cerebellar disease. *Neurology* 1998; 51: 923.
- Sharott A, Marsden J, Brown P. Primary orthostatic tremor is an exaggeration of a physiological response to instability. *Mov Disord* 2003; 18: 195–9.
- Song X-W, Dong Z-Y, Long X-Y, Li S-F, Zuo X-N, Zhu C-Z, et al. REST: a toolkit for resting-state functional magnetic resonance imaging data processing. *PLoS One* 2011; 6: e25031.
- Thompson PD, Rothwell JC, Day BL, Berardelli A, Dick JP, Kachi T, et al. The physiology of orthostatic tremor. *Arch Neurol* 1986; 43: 584–7.
- Timmermann L, Gross J, Dirks M, Volkmann J, Freund H-J, Schnitzler A. The cerebral oscillatory network of parkinsonian resting tremor. *Brain J Neurol* 2003; 126: 199–212.
- Tohka J, Zijdenbos A, Evans A. Fast and robust parameter estimation for statistical partial volume models in brain MRI. *Neuroimage* 2004; 23: 84–97.
- Wills AJ, Thompson PD, Findley LJ, Brooks DJ. A positron emission tomography study of primary orthostatic tremor. *Neurology* 1996; 46: 747–52.
- Wu YR, Ashby P, Lang AE. Orthostatic tremor arises from an oscillator in the posterior fossa. *Mov Disord* 2001; 16: 272–9.
- Xuan Y, Meng C, Yang Y, Zhu C, Wang L, Yan Q, et al. Resting-state brain activity in adult males who stutter. *PLoS One* 2012; 7: e30570.
- Yaltho TC, Ondo WG. Thalamic deep brain stimulation for orthostatic tremor. *Tremor Hyperkinetic Mov* 2011; 1: tre-01-26-56-2.
- Yaltho TC, Ondo WG. Orthostatic tremor: a review of 45 cases. *Parkinsonism Relat Disord* 2014; 20: 723–5.
- Yang H, Long X-Y, Yang Y, Yan H, Zhu C-Z, Zhou X-P, et al. Amplitude of low frequency fluctuation within visual areas revealed by resting-state functional MRI. *Neuroimage* 2007; 36: 144–52.

- Yarkoni T, Poldrack RA, Nichols TE, Van Essen DC, Wager TD. Large-scale automated synthesis of human functional neuroimaging data. *Nat Methods* 2011; 8: 665–70.
- Yelnik J, Bardinet E, Dormont D, Malandain G, Ourselin S, Tandé D, et al. A three-dimensional, histological and deformable atlas of the human basal ganglia. I. Atlas construction based on immunohistochemical and MRI data. *Neuroimage* 2007; 34: 618–38.
- Yin W, Lin W, Li W, Qian S, Mou X. Resting state fMRI demonstrates a disturbance of the cerebello-cortical circuit in essential tremor. *Brain Topogr* 2016; 29: 412–8.